Raman Spectroscopy of Small Para-H_2 Clusters Formed in Cryogenic Free Jets

G. Tejeda,[1] J. M. Fernández,[1] S. Montero,[1] D. Blume,[2] and J. P. Toennies[3]
[1]*Instituto de Estructura de la Materia, CSIC, Serrano 121, E-28006 Madrid, Spain*
[2]*Department of Physics, Washington State University, Pullman, Washington 99164-2814, USA*
[3]*Max-Planck-Institut für Strömungsforschung, Bunsenstraße 10, D-37073 Göttingen, Germany*
(Received 11 February 2004; published 2 June 2004)

Small para-H_2 clusters $(pH_2)_N$ with $N = 2, \ldots, 8$ have been identified by Raman spectroscopy in cryogenic free jets of the pure gas, near the $Q(0)$ Raman line of the H_2 monomer. The high resolution in space, time, and number size makes it possible to follow their growth kinetics with distance from the orifice. At lower source temperatures liquid clusters appear early in the expansion and then undergo a gradual phase transition to the solid state. The technique is very promising for exploring superfluidity in pure $(pH_2)_N$ clusters.

DOI: 10.1103/PhysRevLett.92.223401 PACS numbers: 36.40.–c, 33.20.Fb, 61.46.+w

With only two electrons in a closed shell, H_2 is the simplest and the fundamentally most basic of all molecules. It is also the most prevalent molecule in the Universe. On Earth it is involved in many chemical processes and has recently become of enormous relevance for future energy supply chains. Furthermore, in the nuclear spin modification called para-H_2 (pH_2) it is considered to be the only natural occurring particle in addition to the He atom isotopes, which might exhibit superfluidity [1]. At low temperatures it is in the ground rotational state $J = 0$ and thus like ^{4}He is a spinless boson. Moreover, because of its low mass and weak van der Waals potential it is expected to exhibit extensive quantum delocalization.

The major obstacle to observing superfluidity of H_2 is that the transition temperature, most recently estimated at about 2 K [2], is far below the triple point at 13.96 K. Since it has not been possible to supercool 100–500 μm drops much below the triple point [3], new strategies have recently been developed to overcome the solidification problem. One approach involves a rapid supercooling of the liquid which is best achieved in free jet expansions [4]. Another option is to reduce the coordination by, e.g., studying clusters with fewer than about 20 molecules, which are predicted to exhibit a transition to a superfluid phase at about 2 K [5]. Because of their reduced dimensions the clusters formed are expected to be less prone to both homogeneous [6] and heterogeneous nucleation [7]. So far, however, there is no *direct* experimental evidence of superfluidity of small pure pH_2 clusters. The first indirect experimental evidence for pH_2 superfluidity comes from high resolution infrared spectroscopy of single chromophore carbonyl sulfide molecules coated with 17 pH_2 molecules, which is inside an ultracold (0.15 K) ^{4}He droplet [8]. This interpretation has recently been confirmed by path integral Monte Carlo simulations [9]. The coordination may also be reduced in thin films [10] or in confined geometries [11].

The paucity of data on pure H_2 clusters can be explained by the experimental difficulties resulting from the lack of a permanent dipole moment and the small quadrupole moment of the H_2 molecule. Conventional infrared spectroscopy has been restricted to high-pressure long-path absorption cells [12] and has so far only provided spectral information on the dimers. The alternative spectral probe, Raman spectroscopy, is also impaired by its comparatively low sensitivity.

The present experiments demonstrate that small pure pH_2 clusters produced in a cryogenic free jet can in fact be studied by Raman spectroscopy. The first resolved peaks next to the monomer $Q(0)$ line are assigned to clusters with $N = 2, \ldots, 8$ molecules. This assignment is confirmed by a simple perturbative model using many-body pair distribution functions calculated by the diffusion Monte Carlo (DMC) method together with an effective potential. An extrapolation of the assignments suggests magic numbers at $N \approx 13$, 33, and 55. In colder expansions additional broad peaks shifted to significantly lower frequencies indicate the formation of larger liquid clusters. The gradual appearance of a new spectral feature at even lower frequencies with increased distance from the orifice marks the transition of the liquid clusters to a solid phase.

The clusters are formed in a cryogenically cooled free jet, produced by expanding 99.9999% pure H_2, which was converted to about 99% pH_2, from a stagnation pressure of $P_0 \approx 1$ bar into a lower pressure chamber of $\sim$0.006 mbar. The circular thin walled copper orifices have diameters of $D = 35$ or 50 μm. A closed cycle He refrigerator provides a source stagnation temperature T_0 of 24–60 K, regulated to within ± 1 K. The expansion chamber is pumped by a roots pump backed 2000 l/s turbopump. For Raman excitation the beam from an Ar^+ laser, operated in single mode at $\lambda = 514.5$ nm (4 W), is focused down to a diameter of about 14 μm. The region of the jet to be explored spectroscopically is selected by displacing the orifice axially inside the vacuum chamber with an accuracy of better than 1 μm. The Raman signal was collected at 90° by an f:0.95 optical system with magnifying power $\times 10$. It was then focused

onto the spectrometer slit (20 μm) providing a 2 μm spatial resolution along the jet axis. The spectrometer [13], equipped with a 2360 lines/mm holographic 102 × 102 mm^2 grating and a back-illuminated liquid N_2 cooled CCD detector with 1340 × 400 pixels, has a spectral resolution of 0.14 cm^{-1}.

Typically up to ten spectra were recorded and averaged at each reduced distance $\xi = z/D$ (≤ 50) from the orifice. The total measuring time at each ξ was between 4 and 15 min depending on the density in the jet, which is inversely proportional to ξ^2 and varied from $\sim 10^{20}$–$\sim 10^{16}$ cm^{-3}. All the experiments were well within the jet's "zone of silence" since the Mach disk is predicted at $\xi > 260$. The high spatial resolution and the well-known behavior of the flow speed in jet expansions [14] permit the calculation of the time expired at different distances. The ambient monomer gas temperatures T_i at each distance ξ were estimated assuming an isentropic expansion of an ideal monoatomic gas with $\gamma = 5/3$. This is justified both by the negligible Boltzmann factor of the first excited $J = 2$ rotational level at $\Delta E_{\text{rot}} = 510$ K and the negligible amount of heat released in the condensation of the small ($\approx 1\%$) mole fraction of clusters.

Figure 1 shows a series of Raman spectra measured at five different reduced distances along the center line of the expansion. The peak at 4161.18 cm^{-1} is the $Q(0)$ line of the pH_2 monomer with an (off-scale) signal of ~ 140 photons/s at $\xi = 24$. The small peak at 4155.25 cm^{-1}, marked by an asterisk, is due to the remaining ($<1\%$) fraction of ortho-H_2 in the jet. Each of the satellite peaks next to the pH_2 monomer line can be assigned to clusters of a specific size N. In Fig. 1, dimers appear already at $\xi = 1$. Then at $\xi = 3$ the trimers, tetramers, and pentamers are clearly visible. Only two nozzle diameters further downstream, at $\xi = 5$, a broad peak appears at about 4158 cm^{-1}, which is assigned to $N \approx 13$. Its width suggests an enhanced stability for clusters with sizes near that of the first layer. At much larger distances of $\xi = 24$, with the distribution approaching a steady state, additional broad peaks are observed at $N \approx 33$ (second shell) and at $N \approx 55$ (third shell?). Dividing each peak area in Fig. 1 by N provides a reliable estimate of the concentration of the clusters relative to the monomers. Figure 2(a) shows the time evolution of the mole fractions of the small clusters with $N \leq 6$. Figure 2(b) shows the distribution at $\xi = 10$, not too different from the log-normal distribution [15] expected in the asymptotic region.

Much larger clusters are found at a lower source temperature and greater source pressure, as shown in Fig. 3. At $\xi = 4.3$ the maximum in the Raman spectrum is shifted to 4151.5 cm^{-1} close to the dashed line at 4151.9 cm^{-1} for liquid pH_2 at 18 K [16]. The additional shift of this maximum to smaller wave numbers is attributed to a supercooling of the clusters in the later stages of the expansion. Once formed, the clusters are cooled both by evaporation [4] and by the surrounding

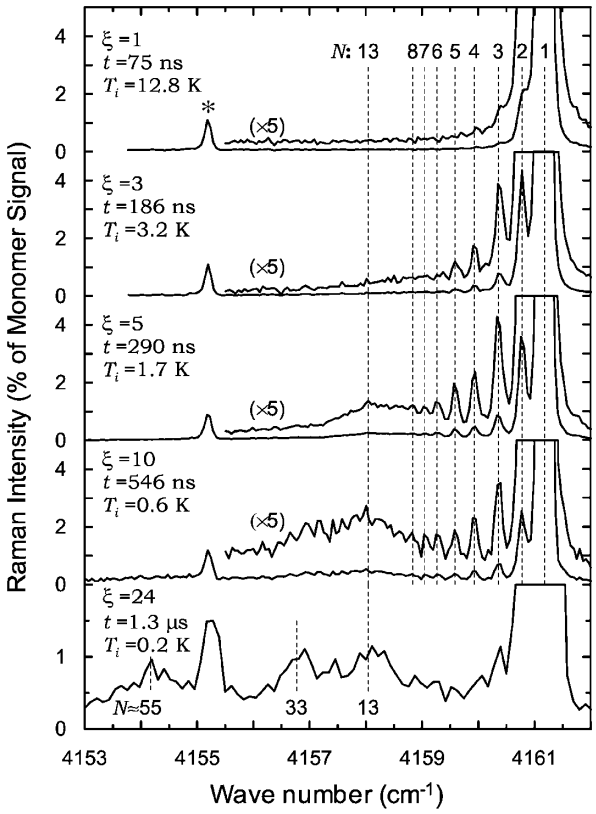

FIG. 1. Raman spectra of small $(pH_2)_N$ clusters in a free jet ($T_0 = 46$ K, $P_0 = 1$ bar, and $D = 50$ μm) as a function of the reduced distance ξ and the flow time t from the orifice; T_i is the estimated isentropic ambient temperature neglecting condensation heating.

gas, which decreases in temperature from about 1.6 to 0.1 K. Since the line shift of the bulk liquid below the triple point at 13.96 K cannot be measured in the bulk, the effect of the lowered temperature can only be deduced indirectly. A similar spectral shift has been reported for

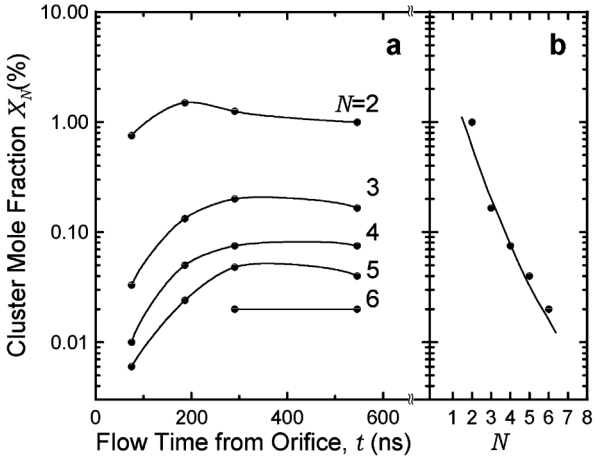

FIG. 2. (a) Time evolution of the size distribution of small $(pH_2)_N$ clusters (source conditions as in Fig. 1). The curve in (b) is a best fit log-normal distribution at $t = 546$ ns. The equilibrium dimer mole fraction in the source is estimated to be only 0.0016%.

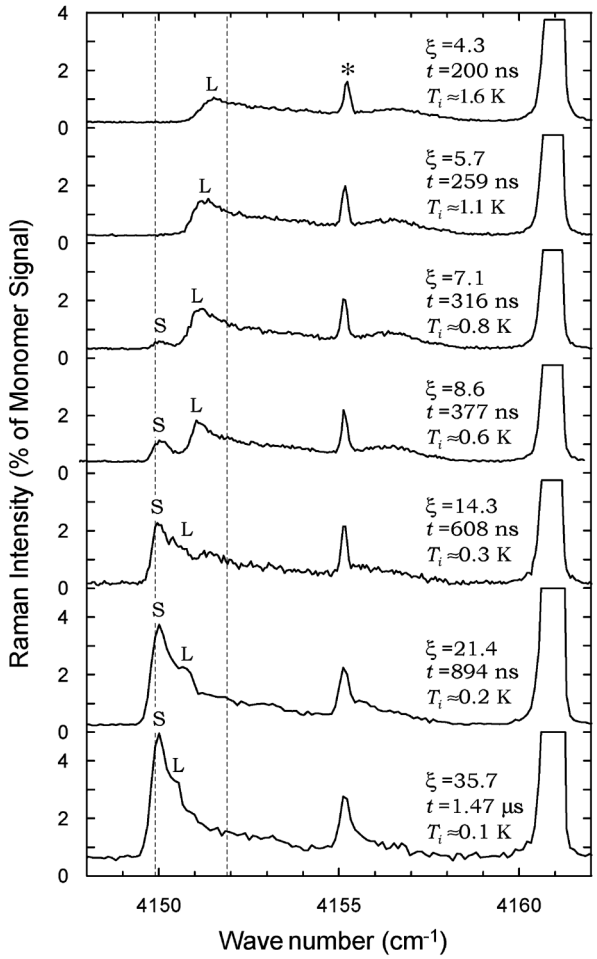

FIG. 3. Raman spectra of large $(pH_2)_N$ clusters as a function of the reduced distance ξ from the orifice. Source conditions: $T_0 = 36.5$ K, $P_0 = 2$ bar, and $D = 35$ μm. S and L stand for solid and liquid, respectively.

supercooled liquid N_2 clusters [17]. It is also expected for other liquids due to the enhanced order and coordination at lower temperatures. In addition to the liquid peak (L) at $\xi = 7.1$, a new peak (S) appears at 4150 cm^{-1}, which agrees with the spectrum for the solid at 2 K [16]. At larger distances the "solid" peak (S) increases in intensity, but since the liquid peak (L) remains about the same it appears that the clusters continue to grow out to the largest distances of $\xi = 36$ explored in these experiments.

To substantiate the line assignments, the spectral shift $\Delta\nu^{(N)} = \delta E_1^{(N)} - \delta E_0^{(N)}$ was calculated from the perturbations of the first excited and the ground vibrational states in the cluster, $\delta E_1^{(N)}$ and $\delta E_0^{(N)}$, respectively. The spectral shift can be estimated assuming a Lennard-Jones–type interaction, $(aR^{-12} - bR^{-6})(q_i + q_j)$, modulated by the normal modes q_i and q_j of every pair of vibrating molecules separated by a distance R. Integrating over the pair distribution function $P^{(N)}(R)$ in the cluster leads to

$$\Delta\nu^{(N)} = (N-1)\int_0^\infty (\alpha R^{-12} - \beta R^{-6}) P^{(N)}(R) dR, \quad (1)$$

where α and β are parameters to be determined. The pair distribution functions $P^{(N)}(R)$ for $N = 2, \ldots, 15$ and 33 were calculated for a spherically symmetric potential [18] using the zero temperature DMC method [19]. The pair distribution functions shown in Fig. 4 indicate that the $(pH_2)_N$ clusters are highly delocalized and floppy. The primary peak of the pair functions at $R \approx 4$ Å depletes as N increases while the tail shifts to larger R values with increasing N, corresponding to the formation of a second shell. The corresponding $g(R)$ function for the bulk liquid [20] is also shown for comparison. The calculated chemical potential reveals a slightly enhanced stability for the $N \approx 13$ clusters, which is supported by a slightly smaller expectation value of the intermolecular distance $\langle R \rangle$. Thus, the $N \approx 13$ clusters are somewhat more compact and stable. The parameters α and β in Eq. (1) were determined from a best fit of the observed line shifts for $N = 2, \ldots, 8$ to be $\alpha = 3.0(3) \times 10^5$ cm^{-1} $Å^{12}$ and $\beta = 2.13(3) \times 10^3$ cm^{-1} $Å^6$.

Table I compares the observed and best fit calculated values of the line shifts and also lists extrapolated values

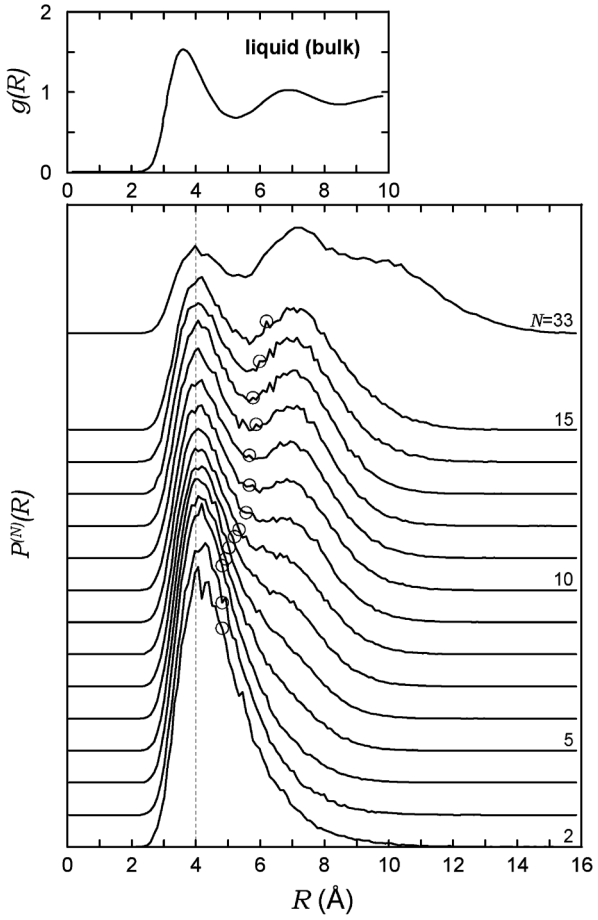

FIG. 4. Pair distribution functions $P^{(N)}(R)$ for $(pH_2)_N$ clusters with $N = 2, \ldots, 15$ and $N = 33$ at $T = 0$, normalized to $\int_0^\infty P^{(N)}(R)dR = 1$, compared with that of the bulk liquid ($N = \infty$) at $T = 20$ K [20]. The circles mark the expectation value $\langle R \rangle$.

TABLE I. Observed and calculated shifts $\Delta\nu^{(N)}$ of $(pH_2)_N$ clusters (in cm^{-1}). Experimental uncertainty (2σ) is 0.02 cm^{-1} for $N = 2, \ldots, 8$, and 0.25 cm^{-1} for $N = 13$ and 33.

N	$\Delta\nu^{(N)}_{obs}$	$\Delta\nu^{(N)}_{calc}$	N	$\Delta\nu^{(N)}_{obs}$	$\Delta\nu^{(N)}_{calc}$	N	$\Delta\nu^{(N)}_{obs}$	$\Delta\nu^{(N)}_{calc}$
2	−0.400	−0.417	5	−1.594	−1.597	8	−2.350	−2.344
3	−0.822	−0.821	6	−1.910	−1.904	13	−3.14[a]	−3.33[b]
4	−1.251	−1.255	7	−2.136	−2.141	33	−4.39[a]	−4.87[b]

[a]Unresolved peaks, not included in the fit of α and β.
[b]Values extrapolated from $N = 2, \ldots, 8$.

for $N = 13$ and 33. The two parameter fit to the experimental line shifts for $N = 2, \ldots, 8$ is excellent and well within the average experimental uncertainty (2σ) of 0.02 cm^{-1}. Also, the extrapolated values agree well with the assumed assignments of the broad peaks at $N \approx 13$ and 33. Moreover, the convergence of the line shifts with increasing N is consistent with the gradual coalescing of the spectral lines which impairs the resolution of distinct peaks in Fig. 1 for $N > 8$.

In summary, small $(pH_2)_N$ clusters with $N = 2, \ldots, 8$ formed in cryogenic free jets have been identified by Raman spectroscopy. Using a simple perturbative model in conjunction with DMC calculated pair distribution functions the observed lines could be described by only two interaction parameters. The good agreement between the experiment and the model calculation provides the first experimental evidence for the highly delocalized nature of these small clusters. Preliminary attempts to calculate the line shifts assuming a rigid [21] structure were unsuccessful. An extrapolation of the model to higher N confirms the assignment of the broad maxima in the spectra to clusters with $N \approx 13$ and 33, and perhaps 55, indicating a propensity for shell structures. The high experimental resolution in space, time, and number size made it possible to follow the growth of individual clusters with unprecedented detail. At the lower source temperatures large liquid clusters are identified and observed to undergo a gradual transition to a solid phase in apparent contradiction with a recent theoretical investigation [6], which rules out solidification under these conditions. The coexistence of a solid and a strongly shifted liquid peak at large distances (Fig. 3) suggests that the predominantly solid clusters have a significant liquid fraction, possibly located at the surface [7,21].

In the future, lower temperatures can be reached by cooling the nascent $(pH_2)_N$ clusters by expanding in an excess of ^4He. $(pH_2)_N$ clusters coated by an outer layer of helium are expected to have evaporation cooled temperatures of 0.38 K (^4He) or 0.15 K (^3He) [22]. To obtain a definite signature for superfluid behavior will require observing either small differences in the pair distribution functions [23], anomalous rotations of the entire complex [5,8], or Raman scattering from collective excitations as, e.g., found in bulk superfluid liquid helium [24].

This work was supported by the Spanish DGI (MCyT), research project No. BFM2001-2265. D. B. acknowledges support from the Petroleum Research Fund and the NSF. We thank Andrej Vilesov for many stimulating discussions, and David Ceperley and Manfred Ristig for valuable correspondence.

[1] V. L. Ginzburg and A. A. Sobyanin, JETP Lett. **15**, 242 (1972).
[2] V. S. Vorob'ev and S. P. Malyshenko, J. Phys. Condens. Matter **12**, 5071 (2000).
[3] H. J. Maris, G. M. Seidel, and F. I. B. Williams, Phys. Rev. B **36**, 6799 (1987).
[4] E. L. Knuth, F. Schünemann, and J. P. Toennies, J. Chem. Phys. **102**, 6258 (1995).
[5] P. Sindzingre, D. M. Ceperley, and M. L. Klein, Phys. Rev. Lett. **67**, 1871 (1991).
[6] A. C. Levi and R. Mazzarello, J. Low Temp. Phys. **122**, 75 (2001).
[7] E. Knuth, S. Schaper, and J. P. Toennies, J. Chem. Phys. **120**, 235 (2004).
[8] S. Grebenev, B. Sartakov, J. P. Toennies, and A. F. Vilesov, Science **289**, 1532 (2000).
[9] Y. Kwon and K. B. Whaley, Phys. Rev. Lett. **89**, 273401 (2002).
[10] F.-C. Liu, Y.-M. Liu, and O. E. Vilches, Phys. Rev. B **51**, 2848 (1995), and references therein.
[11] D. F. Brewer, J. C. N. Rajendra, and A. L. Thomson, J. Low Temp. Phys. **101**, 317 (1995).
[12] A. R. W. McKellar, J. Chem. Phys. **92**, 3261 (1990).
[13] G. Tejeda, J. M. Fernández-Sánchez, and S. Montero, Appl. Spectrosc. **51**, 265 (1997).
[14] D. R. Miller, in *Atomic and Molecular Beams*, edited by G. Scoles (Oxford University, New York, Oxford, 1988), Vol. I, pp. 14–53.
[15] M. Villarica, M. J. Casey, J. Goodisman, and J. Chaiken, J. Chem. Phys. **98**, 4610 (1993).
[16] S. S. Bhatnagar, E. J. Allin, and H. L. Welsh, Can. J. Phys. **40**, 9 (1962).
[17] R. D. Beck, M. F. Hineman, and J. W. Nibler, J. Chem. Phys. **92**, 7068 (1990).
[18] U. Buck, F. Huisken, A. Kohlhase, D. Otten, and J. Schaefer, J. Chem. Phys. **78**, 4439 (1983).
[19] B. L. Hammond, W. A. Lester, Jr., and P. J. Reynolds, *Monte Carlo Methods in Ab Initio Quantum Chemistry* (World Scientific, Singapore, 1994).
[20] D. Scharf, G. J. Martyna, and M. L. Klein, J. Chem. Phys. **99**, 8997 (1993).
[21] D. Scharf, M. L. Klein, and G. Martyna, J. Chem. Phys. **97**, 3590 (1992).
[22] J. Harms, M. Hartmann, J. P. Toennies, A. F. Vilesov, and B. Sartakov, J. Mol. Spectrosc. **185**, 204 (1997).
[23] D. Ceperley (private communication).
[24] T. J. Greytak, R. Woerner, J. Yan, and R. Benjamin, Phys. Rev. Lett. **25**, 1547 (1970).